Protein Folding Kinetics: Barrier Effects in Chemical and Thermal Denaturation Experiments

Athi N. Naganathan, Urmi Doshi, and Victor Muñoz*

Contribution from the Department of Chemistry and Biochemistry, and Center for Biomolecular Structure and Organization, University of Maryland, College Park, Maryland 20742

Received December 22, 2006; E-mail: vmunoz@umd.edu

Abstract: Recent experimental work on fast protein folding brings about an intriguing paradox. Microsecond-folding proteins are supposed to fold near or at the folding speed limit (downhill folding), but yet their folding behavior seems to comply with classical two-state analyses, which imply the crossing of high free energy barriers. However, close inspection of chemical and thermal denaturation kinetic experiments in fast-folding proteins reveals systematic deviations from two-state behavior. Using a simple one-dimensional free energy surface approach we find that such deviations are indeed diagnostic of marginal folding barriers. Furthermore, the quantitative analysis of available fast-kinetic data indicates that many microsecond-folding proteins fold downhill in native conditions. All of these proteins are then promising candidates for an atom-by-atom analysis of protein folding using nuclear magnetic resonance.[1] We also find that the diffusion coefficient for protein folding is strongly temperature dependent, corresponding to an activation energy of $\sim$1 kJ·mol^{-1} per protein residue. As a consequence, the folding speed limit at room temperature is about an order of magnitude slower than the ~ 1 μs estimates from high-temperature T-jump experiments. Our analysis is quantitatively consistent with the available thermodynamic and kinetic data on slow two-state folding proteins and provides a straightforward explanation for the apparent fast-folding paradox.

Introduction

Common practice in experimental protein folding is to interpret raw experimental data with simple chemical models, which describe the folding process as a series of discrete steps. In its simplest version, folding is treated as a two-state transition in which the protein is either fully unfolded or fully folded. The thermodynamic and kinetic properties of folding are then encased in two parameters: an equilibrium constant and a relaxation rate that corresponds to the sum of the rate coefficients for folding and unfolding.[2,3] The inherent simplicity of such an approach is both its major strength and weakness. On the one hand, it has permitted widespread application to many proteins and hundreds of designed mutants, leading to the idea of two-state folding as an intrinsic property of natural single domain proteins.[4] On the other, two-state behavior implies that the critical intermediate stages in folding are always high in free energy (i.e., there is a free energy barrier separating the folded and unfolded states) and thus cannot be directly resolved by experiment.[5] This severe limitation disappears when folding barriers are low (a few *RT* or less) and tunable by experimental conditions, as theoretical arguments based on condensed matter physics predict.[6]

In recent years, we have witnessed the accumulation of strong empirical evidence in support of a theoretical scenario with low folding barriers. Estimates of the folding speed limit obtained from measurements of the time scales for elementary folding processes[7] indicate that the free energy barriers of slow folding ($\tau > 1$ ms) two-state proteins are marginally high.[8] The scaling of folding rates with protein size also supports folding over small barriers.[9] The thermodynamic folding barriers at the midpoint temperature extracted from differential scanning calorimetry (DSC) experiments for 15 proteins range from negative (downhill) to +8*RT* and strongly correlate with their folding rates at 298 K.[10] The emergence of an additional, faster kinetic phase, which is characteristic of folding over marginal barriers (i.e., near *RT*),[11,12] has been observed in mutants engineered to maximize the folding rate of moderately fast-folding proteins.[13,14] Furthermore, examples of global downhill folding (one-state folding), in which there is no significant free energy barrier even at the midpoint of the unfolding transition, have been described[15] and thoroughly investigated experimentally[10,16,17] and computationally.[18,19] Global downhill folding has also been recently exploited to carry out an atom-by-atom analysis of protein folding by nuclear magnetic resonance.[1]

(1) Sadqi, M.; Fushman, D.; Muñoz, V. *Nature* **2006**, *442*, 317−321.
(2) Tanford, C. *Adv. Protein Chem.* **1968**, *23*, 121−282.
(3) Ikai, A.; Tanford, C. *J. Mol. Biol.* **1973**, *73*, 145−163.
(4) Jackson, S. E. *Folding Des.* **1998**, *3*, R81−R91.
(5) Eaton, W. A. *Proc. Natl. Acad. Sci. U.S.A.* **1999**, *96*, 5897−5899.
(6) Bryngelson, J. D.; Onuchic, J. N.; Socci, N. D.; Wolynes, P. G. *Proteins: Struct., Funct., Genet.* **1995**, *21*, 167−195.
(7) Kubelka, J.; Hofrichter, J.; Eaton, W. A. *Curr. Opin. Struct. Biol.* **2004**, *14*, 76−88.
(8) Akmal, A.; Muñoz, V. *Proteins: Struct., Funct., Bioinf.* **2004**, *57*, 142−152.
(9) Naganathan, A. N.; Muñoz, V. *J. Am. Chem. Soc.* **2005**, *127*, 480−481.
(10) Naganathan, A. N.; Sanchez-Ruiz, J. M.; Muñoz, V. *J. Am. Chem. Soc.* **2005**, *127*, 17970−17971.
(11) Ma, H. R.; Gruebele, M. *J. Comput. Chem.* **2006**, *27*, 125−134.
(12) Naganathan, A. N.; Doshi, U.; Fung, A.; Sadqi, M.; Muñoz, V. *Biochemistry* **2006**, *45*, 8466−8475.
(13) Yang, W. Y.; Gruebele, M. *Nature* **2003**, *423*, 193−197.
(14) Ma, H. R.; Gruebele, M. *Proc. Natl. Acad. Sci. U.S.A.* **2005**, *102*, 2283−2287.

In a parallel front, the wide application of temperature-jump techniques has resulted in the experimental identification of several fast-folding single-domain proteins. These proteins fold in a few microseconds at temperatures near their T_m (midpoint temperature).[7] Relaxation rates as a function of chemical denaturant have also been measured for a few of these proteins (and series of mutants) by performing temperature-jump experiments at various concentrations of denaturing chemicals. The characteristic plot of the logarithm of the relaxation rate versus chemical denaturant concentration of microsecond folding proteins still exhibits chevronlike shape, but is typically much flatter than that of slow folding two-state proteins. Given their short folding times and the arguments outlined above, all of these proteins should have very small or negligible folding barriers.[12] However, thermal and chemical denaturation kinetic data for these proteins have been analyzed with chemical two-state models, which seem to work to a first approximation. This apparent paradox elicits interesting questions. Is the apparent compliance of microsecond folding data with two-state kinetics at odds with the expectation of marginal folding barriers? And if it is not, are there any tracks in the two-state analysis of fast-folding proteins signaling the presence of marginal barriers? Here we address these questions by first analyzing fast-folding kinetic data empirically and then theoretically with a one-dimensional free energy surface approach. From the free energy surface we obtain the thermodynamics directly, whereas the relaxation kinetics are described as diffusion on the free energy surface using a Kramers-like treatment. One-dimensional free energy projections have been proven effective in describing folding computer simulations in the cubic lattice[20] and more recently in off-lattice models.[18] One-dimensional projections have also been successfully applied to the prediction of two-state folding rates from protein structures[21] and to reproduce the complex helix-coil kinetics[22] that was revealed by recent T-jump experiments.[23]

From the inspection of the available microsecond folding kinetic data as a function of temperature and/or chemical denaturant we identify systematic deviations from *bona fide* two-state behavior. We then demonstrate that such deviations are simply explained as direct manifestations of folding via marginal barriers. The free energy barriers that we obtain from the theoretical analysis of microsecond folding proteins are consistent with independent estimates of barrier heights[7,10,13] and suggest that several fast-folding proteins do indeed fold in a downhill fashion in nativelike conditions (e.g., 298 K in the absence of chemical denaturants).

Theoretical Calculations

To describe the effects of temperature and chemical denaturation on the equilibrium and kinetics of protein folding we use a simple one-dimensional free energy surface model that is loosely based on

Zwanzig's one-dimensional protein folding model.[24] Zwanzig's model uses the number of residues in incorrect conformation (S) as the reaction coordinate. Each residue can be in either a correct or incorrect conformation, and the entropy is directly obtained from all the possible combinations for each value of S. Instead, our model uses a property we term nativeness (n) as the reaction coordinate. n is defined as the average probability of finding any residue in nativelike conformations. It is a continuous version of the parameter $(N - S)/N$ in Zwanzig's model (with N being the total number of residues and S the number of residues in incorrect conformation). The definition of n as a probability allows for straightforward calculation of the conformational entropy ($\Delta S^{conf}(n)$) using the Gibbs entropy formula:

$$\Delta S_{res}^{conf}(0) = \Delta S_{res}^{n=0} = S_{res}^{n=0} - S_{res}^{n=1}$$

$$\Delta S_{res}^{conf} = \Delta S_{res}^{n=1} = 0$$

$$\Delta S_{res}^{conf}(n) = -R[n \ln(n) + (1 - n) \ln(1 - n)] + n\Delta S_{res}^{n=1} + (1 - n)\Delta S_{res}^{n=0} \text{ for } n > 0 \text{ and } n < 1 \quad (1)$$

$$\Delta S^{conf}(n) = N\Delta S_{res}^{conf}(n) \quad (2)$$

where $\Delta S_{res}^{n=0}$ reflects the difference in conformational entropy between a residue that is populating all possible non-native conformations and the same residue in the fully native conformation.

In the spirit of mean-field theory, we assume that the folding stabilization energy ($\Delta H°(n)$) is an exponential function of n:

$$\Delta H°(n) = \Delta H_{res}°N[1 + (\exp(k_{\Delta H}n) - 1)/(1 - \exp(k_{\Delta H}))] \quad (3)$$

where $\Delta H_{res}°$ is the stabilization energy per residue.

The one-dimensional free energy surface for folding is directly obtained from

$$\Delta G(n) = \Delta H°(n) - T\Delta S^{conf}(n) \quad (4)$$

In this simple model, the free energy barrier for folding arises from the nonsynchronous decay of conformational entropy and stabilization energy, consistently with energy landscape descriptions of protein folding.[25] The magnitude of the folding barrier can be simply adjusted by changing a single parameter: the exponent of the stabilization energy ($k_{\Delta H}$).

To model the effect of temperature on protein folding we define a heat capacity functional ($\Delta C_p(n)$) that also decays exponentially with n:

$$\Delta C_p(n) = N\Delta C_{p,res}[1 + (\exp(k_{\Delta C_p}n) - 1)/(1 - \exp(k_{\Delta C_p}))] \quad (5)$$

$\Delta C_p(n)$ increases linearly with protein size as it has been observed empirically.[26] The exponent determines the curvature of the heat capacity functional, which controls the value of the heat capacity at the top of the barrier for two-state proteins. Using the entropy convergence temperature (385 K) of Robertson and Murphy[26] as the temperature at which solvation terms to the entropy cancel out, we obtain the following expression for the total entropy (conformational plus solvation):

$$\Delta S(T,n) = \Delta S^{conf}(n) + \Delta C_p(n) \ln(T/385) \quad (6)$$

The folding stabilization energy (eq 3) is then defined at the midpoint

(15) Garcia-Mira, M. M.; Sadqi, M.; Fischer, N.; Sanchez-Ruiz, J. M.; Muñoz, V. *Science* **2002**, *298*, 2191−2195.
(16) Oliva, F. Y.; Muñoz, V. *J. Am. Chem. Soc.* **2004**, *126*, 8596−8597.
(17) Naganathan, A. N.; Perez-Jimenez, R.; Sanchez-Ruiz, J. M.; Muñoz, V. *Biochemistry* **2005**, *44*, 7435−7449.
(18) Zuo, G. H.; Wang, J.; Wang, W. *Proteins: Struct., Funct., Bioinf.* **2006**, *63*, 165−173.
(19) Knott, M.; Chan, H. S. *Proteins: Struct., Funct., Bioinf.* **2006**, *65*, 373−391.
(20) Socci, N. D.; Onuchic, J. N.; Wolynes, P. G. *J. Chem. Phys.* **1996**, *104*, 5860−5868.
(21) Muñoz, V.; Eaton, W. A. *Proc. Natl. Acad. Sci. U.S.A.* **1999**, *96*, 11311−11316.

(22) Doshi, U.; Muñoz, V. *Chem. Phys.* **2004**, *307*, 129−136.
(23) Huang, C. Y.; Getahun, Z.; Zhu, Y. J.; Klemke, J. W.; DeGrado, W. F.; Gai, F. *Proc. Natl. Acad. Sci. U.S.A.* **2002**, *99*, 2788−2793.
(24) Zwanzig, R. *Proc. Natl. Acad. Sci. U.S.A.* **1995**, *92*, 9801−9804.
(25) Onuchic, J. N.; LutheySchulten, Z.; Wolynes, P. G. *Ann. Rev. Phys. Chem.* **1997**, *48*, 545−600.
(26) Robertson, A. D.; Murphy, K. P. *Chem. Rev.* **1997**, *97*, 1251−1267.

temperature leading to the following expression for the total changes in enthalpy as a function of temperature and n:

$$\Delta H(T,n) = \Delta H°(n) + \Delta C_p(n)(T - T_m) \quad (7)$$

It is then straightforward to obtain the one-dimensional folding free energy surface as

$$\Delta G(T,n) = \Delta H(T,n) - T\Delta S(T,n) \quad (8)$$

This treatment of the temperature dependence for folding complies with existing empirical descriptions of thermal protein denaturation.[27]

We model chemical denaturation effects as changes in the total free energy of folding that depend linearly on denaturant concentration following

$$\Delta G(F_D,n) = \Delta H°(n) - T\Delta S(n) - mF_D \quad (9)$$

where $\Delta H°(n)$ corresponds to the folding stabilization energy at the experimental temperature (eq 3) and $\Delta S(n)$ corresponds to the entropy functional at the experimental temperature (calculated using the conformational entropy eqs 1 and 2 for simplicity). In this model, m describes the dependence of the chemical destabilization free energy on nativeness, which we define phenomenologically with the equation

$$m = 1 - [(1 + C)(n^j/(n^j + C))] \quad (10)$$

where C and j are phenomenological parameters. m goes from 1 for $n = 0$ to 0 for $n = 1$ and partitions the chemical destabilization free energy between the folding and unfolding sides of the barrier for two-state proteins in ratios that are consistent with empirical measurements of m_f/m_{eq}.

The relaxation kinetics arising from perturbations in the free energy surface are treated as diffusive following a Kramers-like treatment. To calculate the diffusive kinetics we employ a discrete representation of the free energy surface and the matrix method for diffusion kinetics of Lapidus et al.[28] The effective diffusion coefficient is defined as

$$D(T) = k_0 \exp(-NE_{a,res}/RT) \quad (11)$$

For simplicity k_0 is assumed temperature independent, while all the temperature effects arising from changes in solvent viscosity and internal friction from the protein (or landscape roughness[6]) are embedded in the activation energy per residue ($E_{a,res}$).

Calculation of Free Energy Barrier Heights. Barrier heights are calculated from the free energy surface using a dividing line located at two-thirds of the distance in nativeness between the fully unfolded and native minima. The transition state ensemble is defined as the area centered in the dividing line and with a width of 0.12 (for chemical denaturation) or 0.22 (for thermal denaturation) nativeness. Barriers are then obtained from the ratio between the weighted probability of the ground state (unfolded or native) and the transition state. The transition state ensemble was defined as a fixed region of the free energy surface to allow quantitative comparison between profiles exhibiting a maximum between the two minima (i.e., two-state and marginal barriers) and completely downhill profiles. The width of the transition state ensemble was constrained to ensure changes smaller than RT within the ensemble and then calibrated independently in chemical and thermal denaturation calculations to maximize the agreement between folding–unfolding barrier heights and populations on both sides of the barrier (typically within $0.1RT$).

Normalization of m_{kin} Experimental Values. To compare the experimental chemical midpoint rates versus kinetically determined m-values (m_{kin}) from disparate proteins with the theoretical curve (red

curve in Figure 4a), we used a simple normalization procedure. The general idea is to match the relative slope of the changes in m versus midpoint rates for a mutant series with the appropriate segment of the theoretical curve. The position on the x-axis for each protein dataset was obtained by converting its average rate at midpoint to a free energy barrier using a pre-exponential factor of $1/(20 \mu s)$ at 298 K. The experimental m-values for each protein dataset were then normalized using the expression $(m_{kin}^i/\langle m_{kin}\rangle)y$, where y is the y-axis value in the theoretical curve that corresponds to the average barrier height of the mutant series. m_{kin} values for the proteins and mutants were obtained from the kinetic two-state parameters reported in the literature.
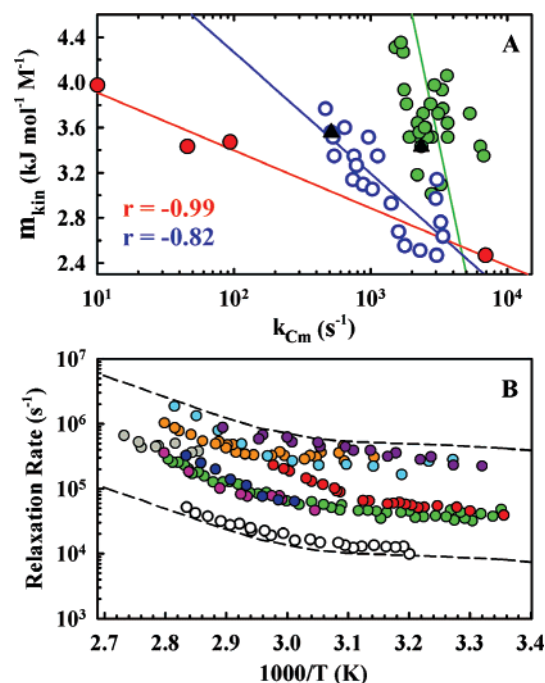
Results and Discussion

Kinetic experiments on fast folding proteins have been systematically analyzed with chemical two-state models.[29−40] The general justification for the two-state analysis is the observation of exponential kinetics. However, exponential decays are not exclusive to high barrier-crossing processes. Some theoretical simulations of the downhill folding regime in simple kinetic models[41,42] and of kinetics over marginal barriers[11,19] produce exponential decays. Diffusive relaxations occurring in a harmonic well in response to the small free energy perturbations characteristic of T-jump experiments also exhibit exponential decays.[43] Moreover, in their analysis of the microsecond-folding 6−85 fragment of λ repressor, Yang and Gruebele noticed deviations from *bona fide* two-state behavior.[37]

In fact, closer inspection of available fast-folding data shows that the deviations from two-state behavior are systematic. In chemical denaturation experiments of microsecond-folding proteins the m-value determined kinetically from the slope of the two limbs of the chevron plot (m_{kin}) seems to be significantly smaller than the m-value from equilibrium experiments (m_{eq}). The trend is quite evident and leads to discrepancies well above experimental uncertainty (~35% lower for m_{kin} in some of the fastest proteins and mutants[31,35,44]). A related phenomenon is the observation of decreasing m_{kin} values as the relaxation rate at the chemical midpoint gets faster in a series of single-point mutants or structural homologues of fast-folding proteins. This effect is illustrated in Figure 1a, which plots the m_{kin} values versus the chemical midpoint rate for the engrailed homodomain family[35] and for mutant series of the E3BD pseudo-wildtype[39]

(27) Freire, E. *Protein stability and folding*; Humana Press: Totowa, New Jersey, 1995.

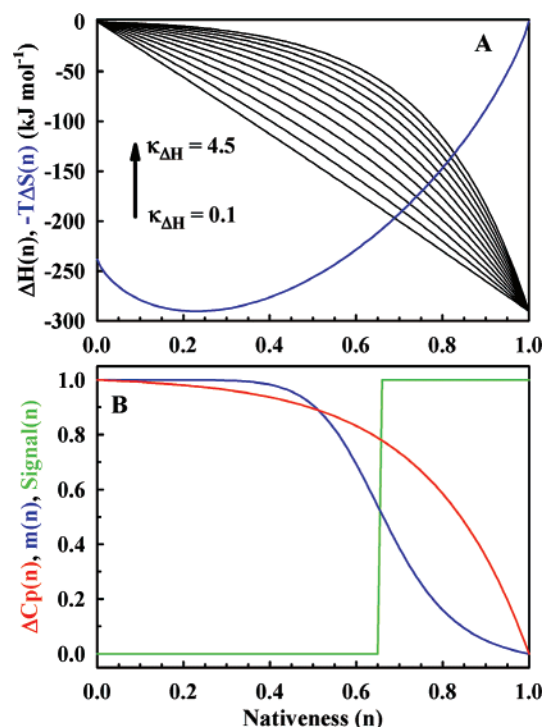(28) Lapidus, L. J.; Steinbach, P. J.; Eaton, W. A.; Szabo, A.; Hofrichter, J. *J. Phys. Chem. B* **2002**, *106*, 11628−11640.

(29) Mayor, U.; Johnson, C. M.; Daggett, V.; Fersht, A. R. *Proc. Natl. Acad. Sci. U.S.A.* **2000**, *97*, 13518−13522.

(30) Jager, M.; Nguyen, H.; Crane, J. C.; Kelly, J. W.; Gruebele, M. *J. Mol. Biol.* **2001**, *311*, 373−393.

(31) Ferguson, N.; Johnson, C. M.; Macias, M.; Oschkinat, H.; Fersht, A. *Proc. Natl. Acad. Sci. U.S.A.* **2001**, *98*, 13002−13007.

(32) Nguyen, H.; Jager, M.; Moretto, A.; Gruebele, M.; Kelly, J. W. *Proc. Natl. Acad. Sci. U.S.A.* **2003**, *100*, 3948−3953.

(33) Kubelka, J.; Eaton, W. A.; Hofrichter, J. *J. Mol. Biol.* **2003**, *329*, 625−630.

(34) Zhu, Y.; Alonso, D. O. V.; Maki, K.; Huang, C. Y.; Lahr, S. J.; Daggett, V.; Roder, H.; DeGrado, W. F.; Gai, F. *Proc. Natl. Acad. Sci. U.S.A.* **2003**, *100*, 15486−15491.

(35) Gianni, S.; Guydosh, N. R.; Khan, F.; Caldas, T. D.; Mayor, U.; White, G. W. N.; DeMarco, M. L.; Daggett, V.; Fersht, A. R. *Proc. Natl. Acad. Sci. U.S.A.* **2003**, *100*, 13286−13291.

(36) Wang, T.; Zhu, Y. J.; Gai, F. *J. Phys. Chem. B* **2004**, *108*, 3694−3697.

(37) Yang, W. Y.; Gruebele, M. *Biochemistry* **2004**, *43*, 13018−13025.

(38) Vu, D. M.; Myers, J. K.; Oas, T. G.; Dyer, R. B. *Biochemistry* **2004**, *43*, 3582−3589.

(39) Ferguson, N.; Sharpe, T. D.; Johnson, C. M.; Fersht, A. R. *J. Mol. Biol.* **2006**, *356*, 1237−1247.

(40) Petrovich, M.; Jonsson, A. L.; Ferguson, N.; Daggett, V.; Fersht, A. R. *J. Mol. Biol.* **2006**, *360*, 865−881.

(41) Muñoz, V. *Int. J. Quantum Chem.* **2002**, *90*, 1522−1528.

(42) Hagen, S. J. *Proteins: Struct., Funct., Bioinf.* **2003**, *50*, 1−4.

(43) Sadqi, M.; Lapidus, L. J.; Muñoz, V. *Proc. Natl. Acad. Sci. U.S.A.* **2003**, *100*, 12117−12122.

(44) Ferguson, N.; Sharpe, T. D.; Schartau, P. J.; Sato, S.; Allen, M. D.; Johnson, C. M.; Rutherford, T. J.; Fersht, A. R. *J. Mol. Biol.* **2005**, *353*, 427−446.

Figure 1. Fast-folding experimental data. (A) Kinetically determined *m*-value (m_{kin}) versus relaxation rate at the chemical midpoint (k_{Cm}) for the engrailed family[35] (red), mutants of E3BD F166W[39] (blue), and mutants of FBP28 WW domain[40] (green). Wild-type proteins are shown as black triangles. Red and blue lines represent linear regression fits while the green line is shown to guide the eye. (B) Folding relaxation rate versus temperature for microsecond-folding proteins. FBP WW domain* ($\Delta N \Delta C$ Y11R-W30F FBP WW;[32] light green), Pin WW domain[30] (white), Villin N27H[33] (cyan), Villin HP36[46] (purple), albumin binding domain (1prb$_{7-53}$ K5I;[36] gray), engrailed homeodomain[29] (red), B-domain of staphylococcal protein A[38] (BdpA; pink), α_3D[34] (orange), and λ_{6-85} D14A[37] (dark blue).

and FBP28 WW domain.[40] Another interesting trend is that the slope for the changes in m_{kin} versus midpoint rate increases with the average rate for the series. In the fastest of the three series (FBP28 WW domain; green in Figure 1a), m_{kin} changes so much relative to the moderate changes in rate that a linear correlation analysis becomes inappropriate. The *m*-value of two-state folding proteins depends on protein size and structure but should be similar for a series of single-point mutants or protein homologues.[45] Furthermore, in two-state folding, any small changes in *m*-value induced by mutation should be uncorrelated with the changes in midpoint rates. Therefore, the trends shown in Figure 1a constitute significant deviations from two-state behavior. The magnitude of the deviations increases with the folding rate, suggesting a direct connection with the height of the folding barrier. This is apparent even for the rates at the chemical denaturation midpoint (Figure 1a) in which barrier heights are maximal (i.e., rates are minimal).

More proteins have been studied as a function of temperature using standard temperature-jump experiments. Figure 1b shows the experimental data for nine of these previously studied fast-folding proteins.[29,30,32−34,36−38,46] The nine fast-folding proteins range from 32 to 80 residues in length (see Table 1), have both α-helical and β-sheet structures, and include the *de novo* designed protein α_3D. The rates at the midpoint temperature (T_m), which averages ∼340 K (see Table 1), are about 1 order

(45) Myers, J. K.; Pace, C. N.; Scholtz, J. M. *Protein Sci.* **1995**, *4*, 2138−2148.
(46) Brewer, S. H.; Vu, D. M.; Tang, Y. F.; Li, Y.; Franzen, S.; Raleigh, D. P.; Dyer, R. B. *Proc. Natl. Acad. Sci. U.S.A.* **2005**, *102*, 16662−16667.

Figure 2. Functionals used in free energy surface analysis of protein folding. (A) Entropic (blue) and enthalpic (black curves) contributions to the free energy. (B) Normalized heat capacity ($\Delta C_p(n)$; red), *m*-value (blue), and fluorescence signal (green) as a function of nativeness.

of magnitude faster than the rates at the chemical midpoint and 298 K. Plotting all the data together reveals very striking similarities. In spite of large differences in size, structure, and sequence, the relaxation rate as a function of temperature is quite similar for all of them. All relaxation rates cluster together within a narrow range at all accessible temperatures (dashed lines in Figure 1b signal a factor of 50). Furthermore, the temperature dependence of the rate is weak and very similar for all the proteins, regardless of their relative folding speed. Accordingly, the rates at T_m of fast-folding proteins correlate with neither size nor the absolute contact order. The relative contact order only shows a marginal correlation coefficient of ∼0.6. In other words, proteins that fold in the microsecond range at their T_m exhibit a strikingly common rate behavior that diverges from that of slower folding proteins. Notably, the apparent temperature dependence of the relaxation rate is not only weak but also almost linear across the accessible temperature range, typically ∼20 K below and above the T_m. This is in contrast with the expectation of opposing temperature dependences for the folding and unfolding limbs in two-state folding.[47] It is also interesting that the rate behavior of Villin HP36 monitored by FTIR[46] and by Trp fluorescence quenching from an engineered Histidine[33] are disparate (purple and cyan circles in Figure 1b), perhaps suggesting the probe-dependent kinetics proposed for proteins near the downhill folding regime.[11]

To rationalize the observations summarized in Figure 1, we employ the simple free energy surface model described above. We simulate chemical denaturation experiments using a cost in entropy of 10 J/(mol·K) per residue, which results in the entropic contribution to the free energy shown in Figure 2a (blue

(47) Oliveberg, M.; Tan, Y. J.; Fersht, A. R. *Proc. Natl. Acad. Sci. U.S.A.* **1995**, *92*, 8926−8929.
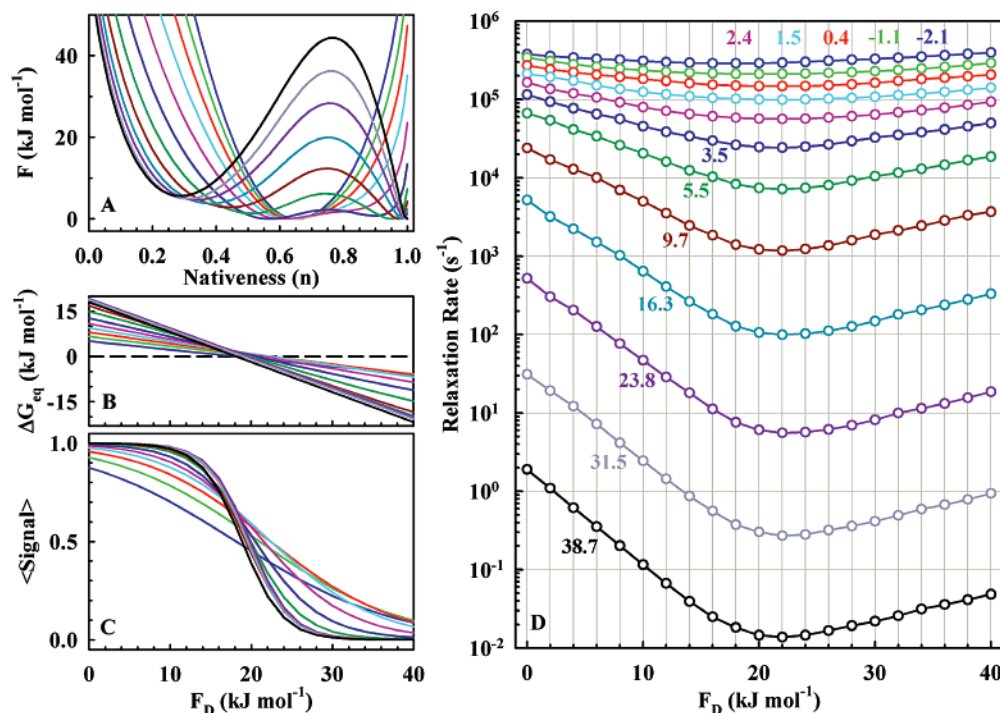
Figure 3. Simulations of chemical denaturation experiments. The coloring scheme corresponds to $\beta_{Midpoint}$ values ranging from -2.1 (blue) to 38.7 (black) kJ·mol^{-1} (see labels in Figure 3d) and is maintained through the figure. (A) Free energy profiles at the chemical midpoint. (B, C, D) Macroscopic stabilization free energy, population weighted signal, and chevron plots, respectively, as a function of the microscopic destabilization free energy (F_D).

curve) for an 80 residue protein. This value is consistent with empirical estimates of the folding entropy at 298 K.[26] The stabilization energy decays exponentially with curvature determined by the magnitude of the exponent (see Figure 2a). The changes in chemical destabilization energy as a function of nativeness are described with the function shown in blue in Figure 2b, which corresponds to eq 10 with coefficients $j = 8$ and $C = 0.04$. This function produces chevron plots with three-fourths of m on the folding limb and one-fourth on the unfolding limb in calculations with high free energy barriers, roughly corresponding to the average values found in two-state proteins. We describe the fluorescence signal of the protein using a one-step function that switches from 0 to 1 at 0.65 nativeness, thus allowing direct simulation of chemical denaturation experiments. Such a one-step function is a reasonable description for the signal expected from a single buried tryptophan[11,41] and maximizes the compliance with two-state behavior by separating the conformational ensemble into two discrete signals (folded and unfolded).

In this model, the magnitude of the entropy cost per residue determines the position and width of the maximum in entropy (blue in Figure 2a), whereas the shape of the free energy surface is determined by the interplay between entropy and enthalpy. For enthalpy functionals with steep curvature (e.g., $\kappa_{\Delta H} > 1.5$ in Figure 2a) the free energy surface at midpoint displays two well-defined minima separated by a high free energy barrier (e.g., black and gray curves in Figure 3a), leading to classical two-state behavior. Enthalpy functionals with shallower decays produce free energy surfaces with only one minimum that moves from high to low nativeness values as the destabilization energy increases (one-state folding[17,41]). At midpoint conditions, the minimum of the one-state free energy surface is located equidistant from the two minima of the two-state cases (e.g., blue curve in Figure 3a). With the enthalpy curves shown in

Figure 2a, the model produces folding barrier heights at the midpoint that range from ~ -2 kJ·mol^{-1} (one-state or global downhill) to ~ 40 kJ·mol^{-1} (Figure 3a), allowing for a detailed exploration of the two-state to one-state folding phase diagram. Our treatment of the chemical destabilization energy results in linear changes in macroscopic folding free energy (i.e., the ratio of the integrated probability on each side of a dividing surface placed at 0.65 nativeness), consistently with experiments.[45] This is the case even for global downhill examples, as is shown in Figure 3b. The simulation of equilibrium chemical denaturation experiments shows typical sigmoidal unfolding curves (Figure 3c). Interestingly, the shape of the equilibrium curve appears insensitive to the folding barrier as long as the barrier height at the chemical midpoint is higher than ~ 10 kJ·mol^{-1} ($\sim 4RT$), but it becomes flatter as the barrier height decreases beyond this point (Figure 3c). Similar behavior is found in the simulation of chemical denaturation kinetic experiments (Figure 3d). All the free energy surfaces shown in Figure 3a, including the global downhill examples, produce V-shaped chevron plots in which the minimum is near the equilibrium denaturation midpoint. This result demonstrates that the observation of chevronlike kinetics is by itself not a diagnostic criterion of two-state behavior. However, the plots become noticeably flatter as the barrier decreases. At first glance, the flattening of the chevron plot shown in Figure 3d is quite similar to the experimental data in the engrailed homeodomain family.[35]

Barrier height effects can be analyzed more specifically by plotting the macroscopic sensitivity to chemical denaturation (relative to the microscopic chemical destabilization free energy; F_D in eq 9) versus the height of the folding barrier at the chemical midpoint (Figure 4a). The macroscopic sensitivity to chemical denaturants is simply obtained by fitting the equilibrium unfolding curves (m_{eq}) or the kinetic chevron plots (m_{kin}) to a chemical two-state model, thereby mimicking the standard
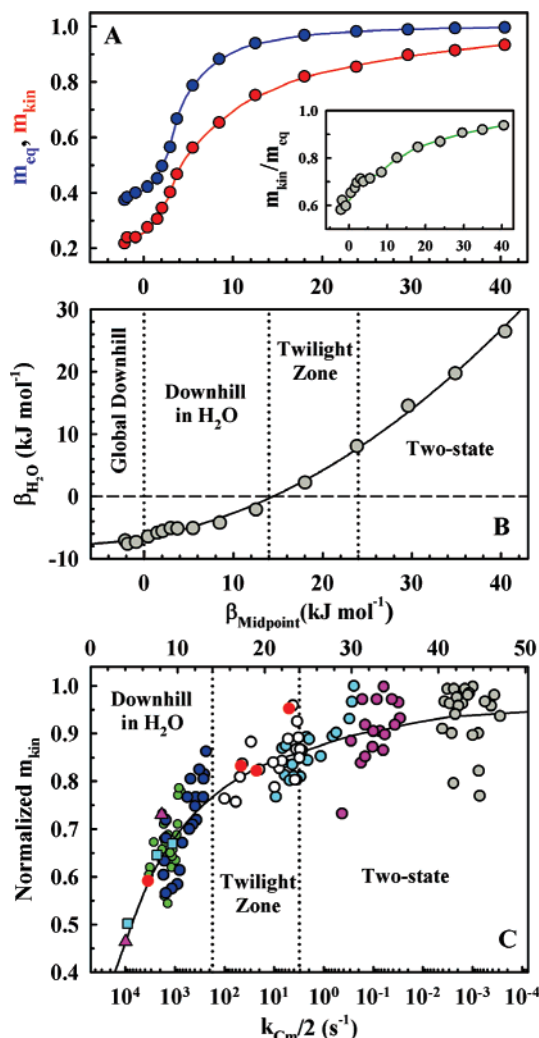
Figure 4. Barrier effects in chemical denaturation experiments. (A) Dependence of equilibrium (blue) and kinetically (red) determined m-values (m_{eq} and m_{kin}) on the barrier height at chemical midpoint ($\beta_{Midpoint}$). The inset plots the m_{kin}/m_{eq} ratio. (B) Plot of the barrier height in water (β_{H_2O}) versus $\beta_{Midpoint}$ showing the four folding regimes. (C) Superimposition of the theoretical m_{kin} curve and normalized experimental data for engrailed family[35] (red circles), BBL-related variants[44] (pink triangles), WW domain family[31] (cyan squares), E3BD F166W[39] (dark blue), FBP28 WW domain[40] (green circles), CspB[49] (white circles), yeast ACBP[50] (cyan circles), L23[52] (pink circles), and muscle AcP[51] (gray circles). The abscissa on the top represents the midpoint barrier heights calculated with a pre-exponential factor of $1/(20 \ \mu s)$.

experimental analysis. The barrier height is calculated directly from the free energy surface (see theoretical calculations). Figure 4a confirms that there are almost no changes in m_{eq} when the barriers at midpoint are ≥ 10 kJ·mol^{-1}. Changes in m_{eq} become increasingly pronounced for barriers between 10 and 0 kJ/mol and taper off for globally downhill proteins. The changes in m_{kin} are more apparent and start at slightly higher midpoint folding barriers (Figure 4a). These results explain the observation of negative correlations between the measured m-value and folding rate at chemical midpoint as well as the increased slope for the faster mutant series (see Figure 1a). Furthermore, Figure 4a shows that this phenomenon is directly linked to folding via marginal folding barriers ($\leq 3.5RT$). Therefore, this analysis indicates that the barriers of microsecond-folding proteins are marginal even at their maximal value (i.e., chemical midpoint). The origin of this behavior is the movement of the minima in

the free energy surface, which tracks the height of the barrier (see Figure 3a). Both minima move closer together as the barrier decrease. However, the shift is much more pronounced for the unfolded minimum, which becomes significantly more structured with lower barriers. Such behavior is in complete agreement with empirical observations of "partly structured" denatured states in fast folding proteins.[31] It is also consistent with a recent phenomenological analysis of folding data, which points to structural changes in the denatured state as the main source for m-value changes upon mutation.[48] It is important to mention here that movement of the minima with the barrier height is an intrinsic property of free energy surface analyses. This property does not depend on the specific formulation of the theoretical model or the parameters employed. It should be a robust property of folding reactions that might be of use to estimate folding barrier heights independently of the magnitude of the diffusion coefficient.

In this regard, the ratio m_{kin}/m_{eq} is of particular interest. m_{kin}/m_{eq} should always be smaller than 1 because barrier effects are stronger on the kinetics (inset of Figure 4a). Therefore, this ratio could be a sensitive indicator of the height of the folding barrier. An additional advantage is that m_{kin}/m_{eq} provides a relative scale that permits direct comparison between different proteins. For proteins with large midpoint barriers m_{kin}/m_{eq} is too close to 1 to permit direct analysis given the accuracy threshold of protein folding experiments. However, for proteins with midpoint barriers ≤ 25 kJ·mol^{-1} the ratio m_{kin}/m_{eq} seems to be small enough to be detectable in standard experimental data. Indeed, the experimental value of 0.89 (no fitting errors available) reported in the literature for the millisecond folding CspB[49] converts into a chemical midpoint barrier of ~24 kJ·mol^{-1}, consistent with its previous assignment to the twilight folding zone based on the analysis of calorimetric data.[10] Literature m_{kin}/m_{eq} values of 0.74 ± 0.06 for engrailed homeodomain,[35] 0.68 ± 0.04 for FBP28 W30A WW domain,[31] and 0.74 ± 0.09 for BBL H166W[44] result in chemical midpoint barrier heights of 6.7 ± 5, 2.1 ± 2.5, and 6.4 ± 8 kJ.mol^{-1}, respectively. In spite of the large uncertainties, the m_{kin}/m_{eq} ratios of these three proteins confirm that their maximal folding barriers (i.e., at the chemical midpoint) are at most marginal. How large are their folding barriers in nativelike conditions? The free energy surface analysis shown in Figure 3 enables us to address this question. Figure 4b shows a plot of the barrier height in nativelike conditions (β_{H_2O}) versus the barrier height at the chemical midpoint. The plot leads to a straightforward classification of the downhill two-state phase diagram into four folding regimes. Two-state proteins are those for which there is a significant barrier (≥ 9 kJ·mol^{-1} or $\sim 3.5RT$) even in nativelike conditions. Proteins with chemical midpoint barriers between 24 and 14 kJ·mol^{-1} are classified as twilight zone because their folding barriers become marginal in native conditions. Finally, the intercept of the 0 barrier line in Figure 4b indicates that proteins with barrier heights ≤ 14 kJ·mol^{-1} at the chemical midpoint should fold downhill in nativelike conditions. The downhill folding group can be divided into two subgroups. The first one corresponds to global downhill proteins in which the barrier is below zero even at the midpoint, as it has been described for BBL.[1,15,17] The second subgroup corresponds to proteins that

(48) Sanchez, I. E.; Kiefhaber, T. *J. Mol. Biol.* **2003**, *327*, 867−884.
(49) Garcia-Mira, M. M.; Boehringer, D.; Schmid, F. X. *J. Mol. Biol.* **2004**, *339*, 555−569.

fold downhill only in native conditions. Therefore, the m_{kin}/m_{eq} analysis indicates that several previously studied microsecond-folding proteins fold downhill in the absence of denaturational stress.

This result can be further tested taking advantage of the dependence of m_{kin} on the midpoint barrier (red curve in Figure 4a). Figure 4a indicates that the slope of the m_{kin} versus midpoint folding rate plot is also sensitive to the barrier height. In principle, matching the curvature of m_{kin} versus midpoint folding rate data from a series of mutants to the theoretical curve in Figure 4a should allow for direct conversion of folding rates into barrier heights, thereby providing estimates of the folding diffusion coefficient for individual protein scaffolds. Unfortunately, the experimental accuracy in the determination of *m*-values is too low for such an exercise. A more practical alternative is to combine mutational data from several proteins spanning a large range in midpoint folding rates using a common (average) folding diffusion coefficient. Because *m*-values strongly depend on protein size, structure, and aminoacidic sequence, the superimposition of data from different proteins requires normalization to the average *m*-value for each mutant series (see the theoretical calculations for details). Figure 4c shows the superimposition of all the experimental data in Figure 1a together with data on two BBL-related variants,[44] three WW domains,[31] and mutational data from two millisecond-folding proteins[49,50] and two slow-folding proteins.[51,52] The curvature of the combined normalized experimental data closely follows the theoretical curve (black curve). Furthermore, this analysis is completely consistent with the m_{kin}/m_{eq} results and indicates that the BBL homologues, the WW domains and their mutants, pseudo-wild-type E3BD and mutants, and engrailed homeo-domain all fold downhill in native conditions. Our free energy surface analysis is remarkably successful in reproducing and interpreting the deviations from two-state behavior observed in chemical denaturation experiments of microsecond-folding proteins.

It is important to notice, however, that the superimposition shown in Figure 4c uses an average folding diffusion coefficient of $1/(20 \mu s)$ at 298 K (compare upper and lower scales in the abscissa of Figure 4c). However, due to the existing data spread, the superimposition is of similar quality for diffusion coefficients ranging from $1/(5 \mu s)$ to $1/(100 \mu s)$. This range of diffusion coefficients is consistent with the value estimated from the comparison between thermodynamic folding barriers estimated from calorimetry and folding rates at 298 K.[10] But, the value of $1/(20 \mu s)$ used in Figure 4c is at least an order of magnitude slower than recent empirical estimates of the folding speed limit from temperature denaturation kinetic experiments.[7] Such empirical estimates are based on experimental data at higher temperature ($\sim$340 K on average), raising the question of whether there is an intrinsic discrepancy between the two values or rather a temperature effect.

To investigate this question we introduce temperature effects in our simple one-dimensional free energy surface model using an implementation that is consistent with existing phenomeno-logical descriptions of folding thermodynamics. In particular, we employ the entropy convergence temperature of Robertson and Murphy (i.e., 385 K) as the temperature at which solvation terms to the entropy cancel out. Under these conditions the entire change in entropy upon folding corresponds to the decrease in conformational entropy.[26] We then use a value of 16.5 $J \cdot mol^{-1} \cdot K^{-1}$ as the difference in conformational entropy between a residue populating all non-native conformations and one in the fully native conformation ($\Delta S_{res}^{n=0}$). This value for $\Delta S_{res}^{n=0}$ results in an average cost in entropy per residue upon folding of $\sim$17.5 $J \cdot mol^{-1} \cdot K^{-1}$ (calculated from the magnitude of the maximum in the conformational entropy functional; eq 1), which coincides with the average change in folding entropy per residue at 385 K estimated from DSC data of 56 two-state proteins.[26] We parametrize the heat capacity functional (eq 5) by directly fitting to this model the DSC data of 14 single-domain proteins, including several proteins that are found to fold downhill by the analysis with the variable-barrier model of Muñoz and Sanchez-Ruiz.[53] All these data could be fitted with an average $\Delta C_{p,res} = 50 \, J \cdot mol^{-1} \cdot K^{-1}$ (also consistent with the empirical analysis of Murphy and Robertson[26]) and $k_{\Delta C_p} = 4.3$. The thermodynamic properties for a given protein are then completely determined by its size (number of residues, *N*) and just two additional parameters: the midpoint temperature (T_m) and the curvature of the enthalpy functional ($k_{\Delta H}$). T_m defines the temperature at which the probability-weighted nativeness ($\langle n \rangle$) reaches a value of $(n_U + n_F)/2$, where n_U and n_F are the nativeness values of the unfolded and folded wells, respectively. The curvature of the enthalpy functional determines the height of the free energy barrier at the midpoint temperature.

Figure 5a shows simulations of temperature-jump kinetic experiments for various examples of 50 residue proteins with $T_m = 335$ K and midpoint barrier heights ranging from -0.6 to 8.2 $kJ \cdot mol^{-1}$ (barrier heights are specified in the legend of Figure 5b). These examples are consistent with the mean protein size and T_m of the set of experimental data shown in Figure 1b. The simulations in Figure 5a have been carried out with a temperature-independent diffusion coefficient and thus illustrate the changes in relaxation rate arising from just the thermodynamic properties of the free energy surface. In these simulations the relaxation rate exhibits a minimum at the midpoint temperature, speeding up at both higher and lower denaturational stress. The origin of the V-shaped rate dependence is that the entropy at the top of the folding barrier is intermediate between the entropies of native and unfolded minima, similarly to *m*-values in chemical denaturation experiments. The heat capacity at the barrier top is also intermediate, producing the characteristic downward curvature of the relaxation rate in native conditions and upward curvature in unfolding conditions.[47] The curvature is less apparent in T-jump experiments and simulations (e.g., Figure 5a) than that in classical stopped-flow experiments at various temperatures[47] simply because of the limited temperature range available to T-jump measurements. A particularly interest-ing trend in the simulations, as we observed before in simula-tions of chemical denaturation experiments, is that the temper-ature dependence of the relaxation rate flattens out as the height of the folding barrier decreases (see Figure 5a). In other words,

(50) Teilum, K.; Thormann, T.; Caterer, N. R.; Poulsen, H. I.; Jensen, P. H.; Knudsen, J.; Kragelund, B. B.; Poulsen, F. M. *Proteins: Struct., Funct., Bioinf.* **2005**, *59*, 80−90.
(51) Chiti, F.; Taddei, N.; White, P. M.; Bucciantini, M.; Magherini, F.; Stefani, M.; Dobson, C. M. *Nat. Struct. Biol.* **1999**, *6*, 1005−1009.
(52) Hedberg, L.; Oliveberg, M. *Proc. Natl. Acad. Sci. U.S.A.* **2004**, *101*, 7606−7611.
(53) Muñoz, V.; Sanchez-Ruiz, J. M. *Proc. Natl. Acad. Sci. U.S.A.* **2004**, *101*, 17646−17651.
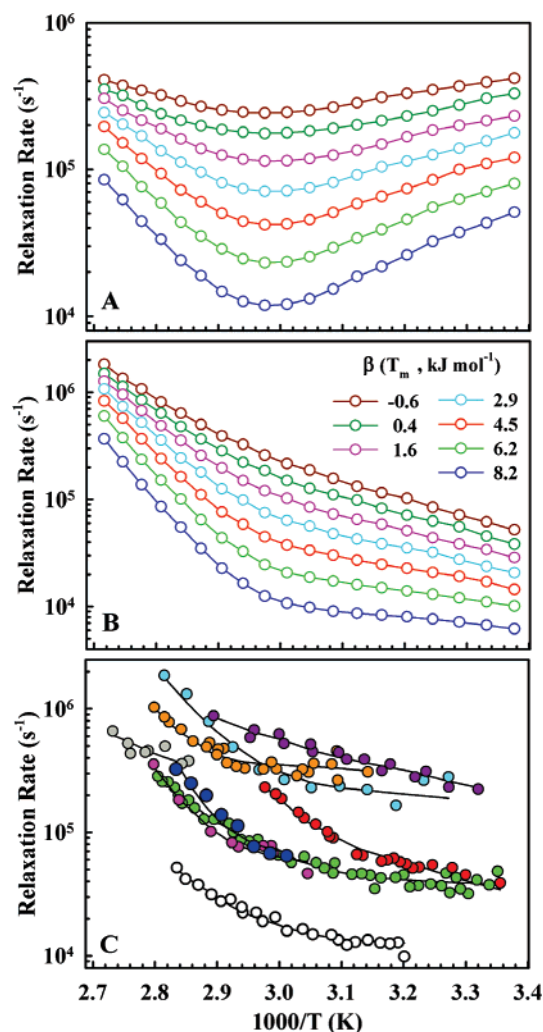
Figure 5. Barrier effects in temperature denaturation experiments. (A and B) Simulated relaxation rate versus temperature for examples of 50-residue proteins with midpoint temperature barrier heights ($\beta(T_m)$) ranging from −0.6 (dark red) to 8.2 (blue) kJ·mol^{-1} in the absence (A) and presence (B) of an activated diffusion coefficient (0.9 kJ·mol^{-1} per residue). (C) Fits (black curves) to the experimental data for the nine microsecond-folding proteins shown in Figure 1b (coloring scheme is maintained).

the free energy surface responds in similar ways to temperature and chemical denaturants.

However, temperature effects on folding kinetics are more complex because the diffusion coefficient is also temperature dependent.[12] In addition to the temperature-induced changes on solvent viscosity, folding diffusion coefficients should include activated terms from the crossing of microbarriers, such as steric hindrance in peptide bond rotations,[54] and from the forming and breaking of non-native interactions as folding proceeds (i.e., roughness in the energy landscape[6,25]). The changes in solvent viscosity correspond to an activation energy of ∼16 kJ·mol^{-1} (∼6.5RT). The activated terms arising from crossing microbarriers and breaking of non-native interactions should scale with protein size because folding dynamics involve concerted motions of the whole polypeptide chain. Moreover, the dynamic terms associated to landscape roughness could exhibit super-Arrhenius temperature dependence.[6,55] Even more complex temperature

effects can arise from the barrier top shifting with temperature together with a diffusion coefficient that depends on the position along the reaction coordinate.[56] For simplicity we describe here the temperature dependence of the diffusion coefficient with a simple Arrhenius activation energy that scales linearly with protein size (see theoretical calculations). An activation term of ∼0.9 kJ·mol^{-1} per residue changes the plots of the relaxation rate as a function of temperature as shown in Figure 5b. This value is consistent with the analysis of the temperature dependence of helix-coil kinetics[54] and with the data shown in Figure 1b (see below). The incorporation of temperature effects on the diffusion coefficient speeds up the relaxation at higher temperatures and slows it down at lower temperatures, resulting in Arrhenius plots that bear striking similarities with the experimental fast-folding data. In spite of the changes introduced by a temperature-dependent diffusion coefficient, the overall trends of Figure 5a remain unaltered. Particularly, it is obvious from Figure 5b that the shape of the relaxation rate versus temperature plot is directly connected to the folding barrier height at the midpoint temperature. Small barriers result in an almost flat relaxation rate below T_m and a highly activated one above it (e.g., blue curve in Figure 5b). The more downhill the protein, the more linear the plot of the relaxation rate versus temperature (e.g., dark red curve in Figure 5b). Thus, combining experimental data on the magnitude and temperature dependence of the relaxation rate allows estimating both barrier height and diffusion coefficient.

We then used the free energy surface model to directly fit the temperature-dependent relaxation rate of all microsecond-folding proteins shown in Figure 1b. The fits involve only four parameters: two that control the properties of the free energy surface (T_m and $k_{\Delta H}$) and two that determine the diffusion coefficient (k_0 and $E_{a,res}$). The model is able to fit the experimental data as well as the two-state models used originally by the authors (Figure 5c), with the advantage that it provides estimates for the folding barrier and diffusion coefficient as a function of temperature. The results of the fitting exercise are summarized in Table 1. The table shows that the activation energy per residue is very similar for most of these proteins and clusters around a value of ∼1 kJ·mol^{-1}. The notable exception is the *de novo* designed protein α_3D, which exhibits a much weaker temperature dependence.

The barrier heights at the T_m are in general small, with several proteins in the 5 to 8 kJ·mol^{-1} range and two proteins with barriers below RT. 1Prb appears to fold globally downhill, in agreement with results from computer simulations.[57] Barriers in Table 1 are upper estimates because a $\Delta C_{p,res} = 50$ is likely to overestimate the heat capacity of very small proteins. The table also shows the values obtained for the minimal folding time (i.e., inverse of the folding speed limit) at the midpoint temperature, which are slightly different from those of the various proteins resulting in a median value of $1/(2.5\ \mu s)$ at $T \approx 340$ K. Such a median value is consistent with recent empirical estimates of the folding speed limit.[7,9] Moreover, the speed limits at T_m that we obtain here for the fast-folding mutant of lambda repressor and for the N27H mutant of Villin headpiece are in very close agreement with the estimates made by the authors with independent methods.[13,58] Another interest-

(54) Thompson, P. A.; Muñoz, V.; Jas, G. S.; Henry, E. R.; Eaton, W. A.; Hofrichter, J. *J. Phys. Chem. B* **2000**, *104*, 378−389.
(55) Zwanzig, R. *Proc. Natl. Acad. Sci. U.S.A.* **1988**, *85*, 2029−2030.

(56) Best, R. B.; Hummer, G. *Phys. Rev. Lett.* **2006**, *96*, 2281041−2281044.
(57) Takada, S. *Proteins: Struct., Funct., Genet.* **2001**, *42*, 85−98.

Table 1. Parameters from the Free Energy Surface Analysis of Thermal Denaturation Kinetics in Microsecond-Folding Proteins[a]

protein	length (N)	$k_{\Delta H}$	$E_{a,res}$ (kJ·mol⁻¹)	T_m (K)	β (T_m)	τ_{min} (T_m)	β_F (298 K)	β_U (298 K)	τ_{min} (298 K)
FBP WW domain*	32	1.54	0.77	327	7.7	2.2	4.1	10.1	5.5
Pin WW domain	34	1.52	0.76	332	6.8	9.8	2.5	10.0	32.9
Villin N27H	35	1.28	1.22	334	6.9	0.5	0.7	11.8	4.7
Villin HP36	36	0.52	0.88	335	0.5	2.8	−3.3	3.0	4.5
$1prb_{7-53}$ K5I	47	1.08	1.15	369	−3.1	1.5	−12.7	3.3	30.8
Engrailed	52	0.75	1.07	325	5.8	2.5	1.4	8.9	17.2
BdpA	58	1.46	1.07	346	5.6	2.8	−4.5	12.6	57.2
α_3D	73	1.05	0.55	346	1.6	2.6	−8.6	9.2	5.4
λ_{6-85} D14A	80	1.36	0.99	346	5.9	2.3	−6.6	14.5	80.4

[a] Minimum folding times (τ_{min}) are given in microseconds, and β values are given in kJ·mol⁻¹.

ing observation is that the results obtained for Villin headpiece are different for the FTIR data of the wild-type sequence[46] and the fluorescence data on the N27H mutant.[33] For Villin N27H we obtain a midpoint barrier of ∼7 kJ·mol⁻¹ and a minimal folding time of 0.5 μs, while for the wild-type the barrier is near zero and the folding time is about 5 times slower. Although the two proteins have similar T_m values and overall rates, the parameters are different because of their distinct temperature dependences (cyan and purple circles in Figure 5c). Differences could arise from the mutation or from the spectroscopic probes employed in these two proteins. Probe dependent kinetics are expected when protein folding involves crossing marginal barriers.[11] But, there also are significant differences in the rate behavior of several single-point mutants of Villin N27H, all of which have been studied using the same fluorescence probe.[33,58] The observation of differences in rate behavior upon single-point mutation is also suggestive of folding over marginal barriers in which the tradeoff between energetic and dynamic contributions to the relaxation rate is delicate. It is interesting that the analysis with a simple one-dimensional free energy surface model is sensitive to such subtle changes in dynamic behavior, suggesting that it can indeed discriminate between slightly different folding behaviors.

Table 1 indicates that the nine microsecond-folding proteins analyzed here have small or no barriers at the midpoint temperature, in agreement with the conclusions extracted from chemical denaturation data. The folding barriers at 298 K are even smaller, with several proteins falling in a clear downhill folding regime (i.e., negative β_F values in Table 1). The remaining proteins fold crossing barriers within RT at 298 K, the only exception being FBP WW domain. Furthermore, the estimates of the minimal folding time at 298 K show quite significant slowdowns, resulting in a median value of 17 μs. The intrinsic errors are larger at 298 K because the parameters are extrapolated from data at very high temperatures for the more stable proteins or correspond to just the relaxation rate for the proteins with negative barrier heights. For example, the two largest minimal folding times in Table 1 (BdpA and λ_{6-85}-D14A) involve long extrapolations and thus could be overestimated. It is interesting to note, however, that a minimal folding time of 80 μs for λ_{6-85}-D14A is consistent with the rate versus temperature data for the pseudo-wild-type and many other mutants of this protein.[37] The only two possible exceptions are mutants Q33A and G46A. For these two mutants two-state estimates of the folding rate at 298 K either from high

temperature[37] or in the presence of chemical denaturants[59] seem to reach values higher than 1/(80 μs), but these estimates also involve long extrapolation. Importantly, the median of the minimal folding times at 298 K, which minimizes biases from extreme values, is in close agreement with the folding speed limit estimated from chemical denaturation data (see above) and with that estimated from the variable-barrier analysis of DSC data.[10] The median value of 17 μs is also similar to the time scales of the fast phase observed during the T-jump-induced renaturation of cold-denatured PGK at 281 K.[60] This fast-phase was assigned by the authors to the diffusive (downhill) formation of a compact globule prior to folding.[60]

Conclusions

Here we introduce a simple one-dimensional free energy surface model of protein folding that is inspired in the basic principles of folding energy landscapes.[6] The implicit assumption in the model is that the order parameter (nativeness, n) is also a reasonable reaction coordinate. Under this assumption the kinetic and thermodynamic folding barriers are identical and completely determined by the free energy surface. The model reproduces quantitatively the chemical and thermal denaturation kinetics of microsecond-folding proteins. This simple model is also consistent with folding thermodynamics and kinetics of slow-folding two-state proteins, including the scaling of thermodynamic parameters with protein size, the value for the conformational entropy at the convergence temperature of Robertson and Murphy,[26] and the temperature dependence of the folding relaxation rate. This indicates that microsecond- and slow-folding proteins follow essentially the same physical principles, which can be captured with a simple phenomenological one-dimensional free energy surface approach.

Furthermore, we can reproduce and rationalize the deviations from two-state behavior that are systematically observed in microsecond-folding proteins. These deviations arise from their folding via marginal barriers even at the denaturation midpoint. The barrier heights and diffusion coefficients that we obtain from chemical and thermal denaturation experiments are consistent with one another and in agreement with independent empirical estimates of folding speed limits[7,9,13,58] and with thermodynamic barriers estimated from the analysis of DSC data.[10] Remarkably, there is also very close agreement between our barrier height estimates and the barriers estimated theoretically and/or computationally for lambda repressor,[61] CspB,[62] and Pin WW domain.[63]

(58) Kubelka, J.; Chiu, T. K.; Davies, D. R.; Eaton, W. A.; Hofrichter, J. *J. Mol. Biol.* **2006**, *359*, 546−553.

(59) Burton, R. E.; Huang, G. S.; Daugherty, M. A.; Fullbright, P. W.; Oas, T. G. *J. Mol. Biol.* **1996**, *263*, 311−322.

(60) Sabelko, J.; Ervin, J.; Gruebele, M. *Proc. Natl. Acad. Sci. U.S.A.* **1999**, *96*, 6031−6036.

Interestingly, our analysis also indicates that many of the microsecond-folding proteins fold in a downhill folding fashion in native conditions (e.g., 298 K in the absence of chemical denaturants). Under such native conditions, the folding barrier is lower than that at the T_m, but the process proceeds significantly more slowly. This is so because the diffusion coefficient includes an activation term, which scales linearly with protein size to a first approximation ($\sim$1 kJ·mol^{-1} per residue). The differences we find between diffusion coefficients and their temperature dependences highlight the inherent difficulties in directly correlating microsecond-folding rates with barrier heights. Since fast-folding proteins are near or within the downhill regime, extreme caution should be exerted in the analysis of mutational data on these proteins. A transition-state analysis, which requires a high free energy barrier to comply with the assumption of instantaneous equilibration between the ground and transition state ensembles,[64] does not appear to be warranted under the fast-folding regime. The good news is that when folding proceeds via marginal (or no) barriers it is possible to extract critical information about the folding free energy surface with a relatively simple analysis, as we show here.

(61) Portman, J. J.; Takada, S.; Wolynes, P. G. *J. Chem. Phys.* **2001**, *114*, 5082–5096.
(62) Plotkin, S. S. *Biophys. J.* **2005**, *88*, 3762–3769.
(63) Cecconi, F.; Guardiani, C.; Livi, R. *Biophys. J.* **2006**, *91*, 694–704.
(64) Hanggi, P.; Talkner, P.; Borkovec, M. *Rev. Mod. Phys.* **1990**, *62*, 251–341.